Novel synergies and isolate specificities in the drug interactions landscape of *Mycobacterium abscessus*

Authors

Nhi Van[1,2], Yonatan N. Degefu[1,2,3], Pathricia A. Leus[1,4], Jonah Larkins-Ford[1,2,4,5], Jacob Klickstein[4], Florian P. Maurer[6,7], David Stone[8], Husain Poonawala[2,8], Cheleste M. Thorpe[2,8], Trever C. Smith II[1,2], Bree B. Aldridge[1,2,4,9]*

Affiliations

[1]Department of Molecular Biology and Microbiology, Tufts University School of Medicine, Boston, MA, 02111

[2]Stuart B. Levy Center for Integrated Management of Antimicrobial Resistance, Boston, MA, 02111

[3]Current: Department of Biomedical Engineering, University of Virginia, Charlottesville, VA, 22904

[4]Graduate School of Biomedical Sciences, Tufts University School of Medicine, Boston, MA, 02111

[5]Current: MarvelBiome, Inc., Woburn, MA 01801, USA

[6]Institute of Medical Microbiology, Virology and Hygiene, University Medical Center Hamburg-Eppendorf, Hamburg, Germany

[7]National and WHO Supranational Reference Center for Mycobacteria, Research Center Borstel, Borstel, Germany

[8]Division of Geographic Medicine and Infectious Diseases, Department of Medicine, Tufts Medical Center and Tufts University School of Medicine, Boston, MA

[9]Department of Biomedical Engineering, Tufts University School of Engineering, Medford, MA, 02155

Author List Footnotes:

Corresponding author(s) e-mail address(es):

*Correspondence: bree.aldridge@tufts.edu

ABSTRACT

Mycobacterium abscessus infections are difficult to treat and are often considered untreatable without tissue resection. Due to the intrinsic drug-resistant nature of the bacteria, combination therapy of three or more antibiotics is recommended. A major challenge in treating *M. abscessus* infections is the absence of a universal combination therapy with satisfying clinical success rates, leaving clinicians to treat infections using antibiotic lacking efficacy data. We systematically measured drug combinations in *M. abscessus* to establish a resource of drug interaction data and identify patterns of synergy to help design optimized combination therapies. We measured approximately 230 pairwise drug interactions among 22 antibiotics and identified 71 synergistic pairs, 54 antagonistic pairs, and four potentiator-antibiotics not previously reported. We found that commonly used drug combinations in the clinic, such as azithromycin and amikacin, are antagonistic in lab reference strain ATCC19977, whereas novel combinations, such as azithromycin and rifampicin, are synergistic. Another challenge in developing universally effective multidrug therapies for *M. abscessus* is the significant variation in drug response between isolates. We measured drug interactions in a focused set of 36 drug pairs across a small panel of clinical isolates with rough and smooth morphotypes. We observed highly strain-dependent drug interactions that cannot be predicted from single-drug susceptibility profiles or known drug mechanisms of action. Our study demonstrates the immense potential to identify synergistic drug combinations in the vast drug combination space and emphasizes the importance of strain-specific combination measurements for designing improved therapeutic interventions.

INTRODUCTION

Mycobacterium abscessus (M. abscessus) is a rapidly growing nontuberculous mycobacterium (NTM) that consists of three subspecies, *M. abscessus* subsp. *abscessus*, *M. abscessus* subsp. *massiliense* and *M. abscessus* subsp. *bolletii* (1). *M. abscessus* is a ubiquitous, opportunistic pathogen commonly found in soil, water systems, and contaminated material in hospitals. Recently, a steady increase in the morbidity and mortality of NTM infections has been reported worldwide (2). Although *M. abscessus* causes both pulmonary and extrapulmonary infection, the majority of the clinical syndrome of *M. abscessus* infections are pulmonary, occurring in immunocompromised people and those with pre-existing conditions such as cystic fibrosis, chronic obstructive pulmonary diseases, and bronchiectasis (3, 4).

Pulmonary *M. abscessus* infections are notoriously hard to treat due to the plethora of intrinsic mechanisms conferring resistance toward most clinically relevant antimicrobials, including macrolides, aminoglycosides, tetracyclines, and ß-lactams (5). Antibiotics such as amikacin and moxifloxacin are bactericidal in *E. coli* but are bacteriostatic in *M. abscessus*, creating another barrier to treating *M. abscessus* infection (6). The inherent phenotypic drug resistance in *M. abscessus* is due to multiple factors. *M. abscessus* possesses complex drug efflux pump system. a cell wall rich in lipids and mycolic acids that act as a physical barrier between antibiotics and the bacteria (7). Additionally, *M. abscessus* express numerous enzymes that can modify drugs or their targets. For example, studies have identified multiple enzymes in *M. abscessus* such as the Erm(41) erythromycin ribosomal methyltransferase, aminoglycoside acetyltransferases, an aminoglycoside phosphotransferase, a rifamycin ADP-ribosyltransferase (Arr_{Mab}), a ß-lactamase (Bla_{mab}), and tetracycline-modifying monooxygenase that confer their ability to resist many clinically used antibiotics (7-9). In addition to intrinsic resistance, acquired mutational resistance against macrolides and aminoglycosides also poses a significant risk for chronically infected patients with increased long-term antibiotic exposure (10). These characteristics contribute to the complex and multifaceted resistome of *M. abscessus*, creating a major challenge in developing antimicrobial therapies against *M. abscessus*.

Despite being an emerging global health threat, pan-effective treatment for NTM lung diseases has not yet been established and current treatment guideline is based on small studies and expert opinion (11, 12). Hence, treatment of *M. abscessus* is highly individualized and typically split into an intensive initial phase of several weeks comprising at least three antibiotics and a continuation phase of several months. In patients infected with strains harboring inducible or mutational resistance to macrolides, a macrolide can be included in the regimen for its immunomodulatory purpose only (12). Current guidelines suggest a minimum treatment duration of twelve months after culture conversion, although it is also individualized based on several factors, such as underlying patient conditions and *M. abscessus* subspecies, which typically have different clinical outcomes (3, 13). Clinical outcomes are poor in patients with pulmonary disease and those with immunosuppression (2, 14). Meta-analysis done across multiple clinical studies showed that sputum conversion without relapse was low, and evidence suggests that surgical resection prolongs negative culture (13, 15, 16). The poor cure rate and the emergence of clinically acquired pan-macrolide and pan-aminoglycoside resistance suggest the urgent need to develop more

effective therapies for NTM and *M. abscessus* infections (8). Except for clarithromycin, results of traditional antimicrobial susceptibility testing by the Clinical and Laboratory Standards Institute (CLSI) are not linked to clinical outcomes (17). Additionally, there are no published breakpoints for tigecycline, or repurposed MDR-TB drugs like clofazimine or bedaquiline that are used to treat *M. abscessus*. Because *M. abscessus* treatment requires multi-drug therapy, systematic interrogation of drug combinations and drug-drug interactions has the potential to identify synergistic combinations that will form the basis for more effective therapies.

Several combination studies for *M. abscessus* have been reported using traditional checkerboard assays. However, conducting large-scale drug combination measurements is not practical because systematic measurements of drug-dose combinations in the checkerboard make these assays too resource-intensive. Here, we utilized DiaMOND (diagonal measurement of n-way drug interaction), a measurement and analysis pipeline based on an efficient geometric sampling of a traditional checkerboard assay, to significantly decrease the number of measurements required in checkerboard assays (18). We modified the DiaMOND assay to measure potentiation effects of drugs that are not active on their own but may increase the efficacy of other compounds. Because there are few antibiotics that are active in *M. abscessus*, potentiator screens may be critical to developing combination therapies in *M. abscessus* and other NTMs. Using medium-throughput measurement, we generated a systematic, large-scale catalog of drug interactions for *M. abscessus* as a resource and evaluated drug interaction patterns. Our dataset includes antibiotics commonly used in the clinic and next-generation antibiotics, such as bedaquiline or benzimidazole SPR719, an active moiety of a non-fluoroquinolone gyrase inhibitor SPR720. We identified many novel synergistic drug pairs, suggesting the potential for effective multidrug regimens in the combination drug space. However, drug interactions were highly variable among different clinical isolates highlighting the importance of making isolate-specific drug combination measurement rather than searching for a universal drug combination to treat *M. abscessus* infection.

RESULTS

Design of systematic drug interaction study in ATCC19977

To generate a systematic dataset of drug interaction profiles comparable to other published drug interaction studies, we began by measuring drug combination responses in the *M.*

126 *abscessus* reference strain ATCC19977, an *M. abscessus* subsp. *abscessus* variant showing
127 inducible macrolide resistance due to a functional Erm(41) ribosomal methylase (19). We
128 measured pairwise combination effects among 22 antibiotics drawn from four categories
129 (Table 1): **(a)** antibiotics currently recommended for *M. abscessus* treatment such as
130 amikacin, clarithromycin, and azithromycin, **(b)** anti-tuberculosis drugs such as linezolid and
131 ethambutol, **(c)** drugs in development for *M. abscessus* infection such as bedaquiline and
132 SPR719, and **(d)** drugs that show no significant effect on their own but can be used to
133 potentiate other drugs, such as avibactam.

Table 1. Summary of antimycobacterial used in the study and their antimicrobial activity against *M. abscessus* ATCC19977

	antimycobacterial	general mechanism of action	abbreviation	IC_{50} (µg/mL)	IC_{90} (µg/mL)
active drug	**amikacin**	protein synthesis	AMK	6.6	110
	amoxicillin	cell wall	AMX	300	NA
	azithromycin	protein synthesis	AZM	4.3	680
	bedaquiline	respiration	BDQ	0.16	1.3
	cefoxitin	cell wall	FOX	9	28
	cerulenin	cell wall	CER	2.2	7
	clarithromycin	protein synthesis	CLR	0.45	80
	ethambutol	cell wall	EMB	31	1200
	levofloxacin	DNA	LXF	13	200
	linezolid	protein synthesis	LZD	14	260
	moxifloxacin	DNA	MXF	1.5	35
	nitrofuran	DNA	NFT	44	1800
	rifabutin	RNA	RFB	1.8	23
	rifampicin	RNA	RIF	16	2100
	SPR719	DNA	SPR	0.39	NA
	telithromycin	protein synthesis	TEL	10	NA
	thioridazine	respiration	TZ	23	39
	vancomycin	cell wall	VAN	9	250
potentiator	***avibactam***	ß-lactamase inhibitor	AVI	NA	NA
	streptomycin	RNA	STR	NA	NA
	tetracycline	RNA	TET	NA	NA
	verapamil	efflux pump inhibitor	VER	NA	NA

Drug combinations may be constructed from antibiotics that are active on their own and are effective together. We may then search for synergistic drug combinations, e.g., sets of antibiotics that are more effective together than expected based on their single-antibiotic efficacies. Nevertheless, applying this approach systematically to *M. abscessus* poses a challenge due to its inherent drug resistance and the large-scale, resource-intensive, traditional checkerboard assays. To overcome the latter, we used DiaMOND to measure pairwise combination effects more efficiently. DiaMOND is an experimental analysis method approximating the checkerboard assay to measure drug interactions. The first step of DiaMOND is to determine the 50% and 90% growth inhibitory concentrations (IC_{50} and IC_{90}, respectively) of every drug to design an equipotent combination dose-response curve. We sampled 20-25 doses to obtain a dose-response curve for every drug. From obtained IC_{50}

values, we designed pairwise DiaMOND experiments for equipotent combinations of drug pairs (diagonal in Fig. 1A). Fractional inhibitory concentrations at 50% growth inhibition (FIC_{50}) were calculated based on Loewe Additivity and Bliss Independence null models. Metrics from both models were strongly correlated (R^2 = 0.75, Pearson correlation), so we focused on FICs calculated by Loewe Additivity (Fig. S1). We report $\log_2$FIC values, such that synergies (negative) are balanced in magnitude compared to antagonisms (positive). We can also visualize synergies and antagonisms by comparing combination dose-response curves to single drug dose-response curves (Fig. 1C)

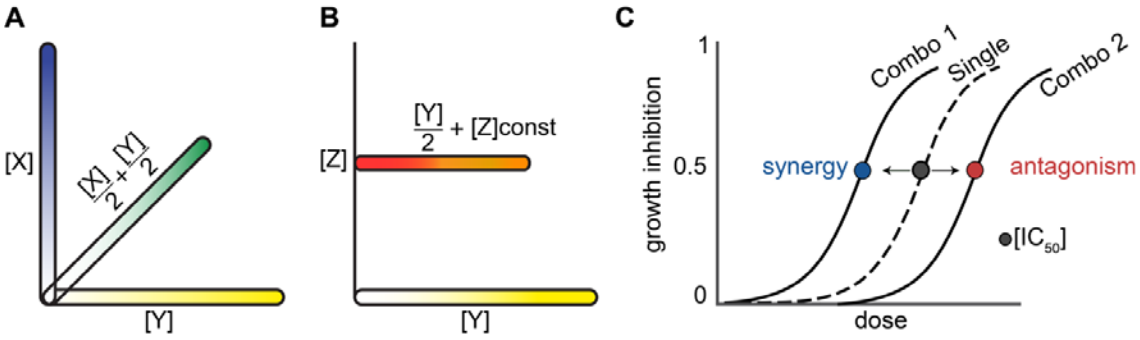

FIG 1. Schematic of drug interaction and potentiation measurement with DiaMOND. (A) DiaMOND single (axes) and pairwise (diagonal) dose-response sampling using an equipotent mixture of two drugs. The x- and y-axes show the doses of the single drugs (X and Y) sampled from low to high concentrations, as indicated by the blue and yellow gradient. The diagonal is the mixture of half of each single drug at each dose, as shown by the green gradient. (B) Schematic of antibiotic and antibiotic-potentiator dose-response measurement. A dose-response for the antibiotic alone (Y; yellow gradient) and with the addition of a constant concentration of the potentiating agent (Z; red to orange gradient). The antibiotic-potentiator dose-response is a mixture of half the dose of the potentiating drug (constant) and half of the non-potentiating drug (increasing amounts in a dose-response). (C) Schematic of shifts in dose-response curves with synergy or antagonism. The dose-response curve in the dashed line represents the effect of a single drug. When the single drug is combined with another drug, the combination curve might shift to the left, indicating synergy (blue dot), or shift to the right indicating antagonism (red dot).

Another complementary approach is to design combinations that include potentiators, e.g., inactive compounds as single agents that increase the efficacy of other drugs. Similarly, an inactive drug can also decrease the efficacy of other drugs, and we refer to this effect as

attenuation. This approach could be particularly relevant in designing combination therapy against *M. abscessus*, where there is a dearth of potent antibiotics for clinicians to choose from. For example, SPR741, a synthetic polymyxin analog with little effective against gram-negative bacteria as a stand-alone agent, exhibits synergy in combination with other antibiotics (20-22). In *M. abscessus*, verapamil has minimal activity against ATCC19977 but potentiates the activity of bedaquiline (23). Another reason to search for potentiator-antibiotic pairs is the possibility of reducing treatment doses to alleviate side effects. For instance, intravenous amikacin can cause adverse effects, including gastrointestinal distress (e.g. nausea) and serious cases of ototoxicity and nephrotoxicity (24). A partner drug to amikacin that potentiates its activity could lower the treatment dose and reduce adverse effects.

DiaMOND was initially designed to quantify drug interaction between two potent drugs. Therefore, modification is required to quantify drug interaction between an active drug and a potentiator candidate. Here, we defined potentiator candidates as compounds that did not achieve growth inhibition at a clinically achievable concentration in patients without extreme adverse side effects. We have included four potentiator candidates in our study: avibactam, tetracycline, streptomycin, and verapamil (Table 1). Because potentiator candidates are not active as single drugs, we developed a geometrically optimized sampling of the checkerboard assay to measure the effect of the potentiator candidate at a constant dose on the potency of effective (dose-responsive) antibiotics (Fig 1B). We measured two-dose responses: (a) the single-drug dose-response curve [Y] with increasing concentrations and (b) the single-drug dose-response [Y] (in which drug concentration was reduced by half for all doses) combined with a fixed-dose (1.5x reported maximum plasma concentration after 12-24 hours of dosing in humans) of drug [Z] (Fig. 1B) (25). The effect of the potentiator candidate was calculated as a fold change in concentration of the antibiotic to reach a specific level of growth inhibition (IC_{50} or IC_{90}) with the potentiator candidate compared to the drug alone. This fold shift in IC (FsIC) ratio can be interpreted similarly to FIC values: $\log_2$FsICs are negative for potentiator-drug pairs and positive for attenuator-drug pairs. We focused on evaluating fold shifts at 50% and 90% growth inhibition levels ($FsIC_{50}$ and $FsIC_{90}$, respectively). Potentiation and attenuation can be visualized by the shift of combination dose-response curves relative to single-drug dose-response curves resembling synergy and antagonism, respectively (Fig.1C), with the exception that the combination dose-response utilizes a constant dose of the potentiator candidate with an increasing dose level of the antibiotic.

A drug interaction landscape of ATCC19977

To generate a systematic dataset of drug interactions for *M. abscessus*, we measured 153 pairwise combinations of 18 drugs representing five drug classes in the reference strain ATCC19977 (Fig. 2A). Among these combinations, we report 122 combinations that passed our quality control metrics. The details of quality control metrics can be found in the method section. Briefly, passing criteria include metrics such as Z-factor, the quality of the dose-response curve fitting, and data reproducibility. The most common reason for quality control failure was variation in potency that compromised the equipotent design of the combination dose-response curve, leading to poor equipotency score and reproducibility. Interactions were measured up to nine times; combinations that failed to achieve at least biological duplicates that passed these criteria were categorized as unmeasurable and reported as N/A (gray boxes in Fig. 2A) in this dataset. Approximately 20% of the drug interactions were unmeasurable due to extreme variation in drug combination response, which is consistent with challenges in measuring drug susceptibility to *M. abscessus* due to lack of reproducibility (26). Nonetheless, it is important to understand which drug combinations cannot be reliably measured.

To understand how well DiaMOND drug interaction measurements correlate with other independent studies, we compared our measurements with previously reported results. We observed a qualitative (synergy vs. antagonism) agreement between drug interactions from DiaMOND and other studies. For example, bedaquiline has been shown to eliminate the bactericidal effect of ß-lactam by dampening the overproduction of ATP to toxic levels normally found upon treatment with these drugs (27). Using DiaMOND, we observed a mild antagonism (log_2FIC_{50} of 0.25) between bedaquiline and cefoxitin, a ß-lactam (Fig. 2B). The antagonism can be visually observed by the right shift of the combination dose-response curve (solid line), compare to the expected combination dose-response curve if ½ concentration of bedaquiline and ½ concentration of cefoxitin were used (not shown in the figure). Similarly, we observed a mild antagonism between linezolid and moxifloxacin in agreement interactions reported in Zhang et al. (log_2FIC_{50} of 0.67 and 0.17, respectively, Fig. 2C) (28). Combinations such as rifabutin and clarithromycin were reported to be synergistic by Pyrjma et al. (29). Using DiaMOND, we also observed that rifabutin and clarithromycin are synergistic (log_2FIC_{50} of -0.76 and -3.1, respectively**)**. Taken together, we conclude that DiaMOND measurements of *M. abscessus* drug interactions are comparable to traditional checkerboard approaches previously reported in other studies.

In other bacterial species, including *M. tuberculosis* and *E. coli,* drug interactions tend toward antagonism (30). In our study, we observed a tendency toward synergy in the landscape of

drug interactions in *M. abscessus*. Of the 122 measurable pairwise drug interactions among 18 drugs, about two-thirds (71) were synergistic or additive (with ~ 0 and negative $\log_2 FIC_{50}$ values). Our data suggests that there is potential to improve *M. abscessus* multi-drug regimens using combinations of existing antibiotics. To further explore these combinations, we analyzed our dataset in smaller sections for interpretability.

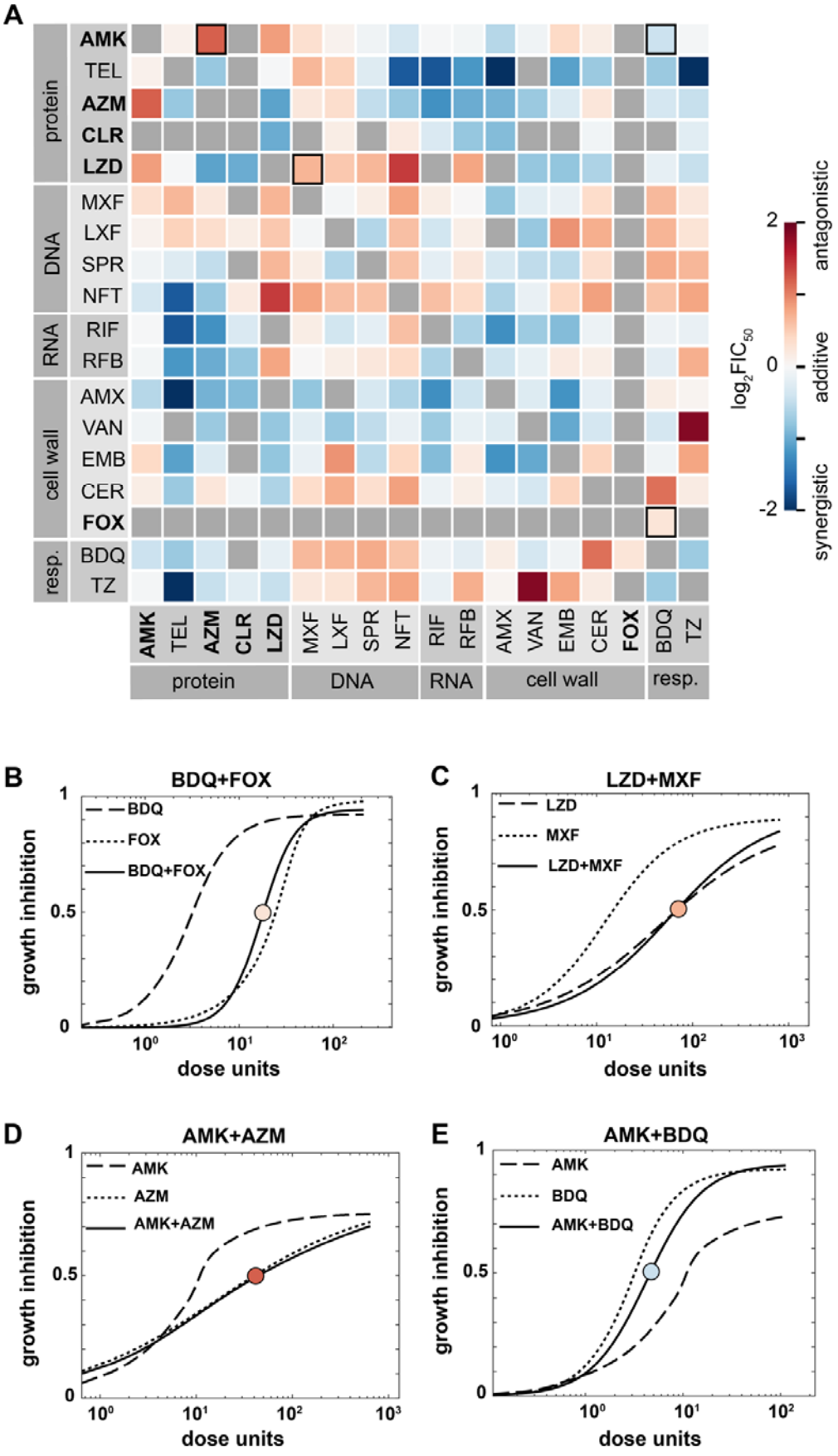

245

FIG 2. Drug interaction landscape of *M. abscessus strain* ATCC19977. (A) Heatmap of pairwise drug interactions among 18 drugs. Drugs are organized by the mechanism of action, and drugs recommended for treating *M. abscessus* infection are indicated in bold text. Drug interactions are evaluated with log_2FIC_{50} values: $log_2FIC < 0$ (synergy, blue) and $log_2FIC > 0$ (antagonism, red). Gray boxes indicate unmeasurable drug combinations due to poor reproducibility. Outlined squares indicate combinations that are shown in the dose responses below. (B-E) Example pairwise (and corresponding single-drug) dose responses. Pairwise dose responses for synergistic and antagonistic combinations are shifted to the left and right, respectively, as compared to the corresponding single-drug dose-response curves. Circles with gray indicate the IC_{50} of single drugs, and circles with the red-blue scale according to log_2FIC_{50} values as in (A). The y-axis represents growth inhibition, whereas the x-axis represents the dose unit (a unitless representation of the volume, or concentration, used for each drug. A dose unit is preferred when plotting as different drugs have different inhibition concentrations, while a dose unit normalizes the difference and allows easy representation) (B-C) Dose-response curves of combinations that were reported from other studies which are bedaquiline (BDQ) + cefoxitin (FOX) (B) and linezolid (LZD) + moxifloxacin (MXF) (C). (D) Dose-response curves for clinically relevant combination amikacin (AMK) + azithromycin (AZM) (antagonistic) and (E) novel combination amikacin (AMK) + bedaquiline (BDQ) (synergistic).

Amikacin and macrolides (azithromycin and clarithromycin): Combination treatment with amikacin and azithromycin (or clarithromycin) is a recommended treatment for macrolide-susceptible *M. abscessus* (12). We observed a strong antagonistic relationship between amikacin and a commonly used macrolide, azithromycin (Fig. 2D, log_2FIC_{50} of 1.2). We also tested another macrolide-amikacin pair (clarithromycin-amikacin) but found that the combination was unmeasurable because the data fluctuated significantly from replicate-to-replicate. Generally, we did not observe any strong synergistic combinations between amikacin and other tested drugs, except with amoxicillin, bedaquiline, and nitrofurantoin (log_2FIC_{50} of -0.58, -0.43, and -0.36, respectively). None of these drugs are currently being recommended to be used with amikacin. For azithromycin and clarithromycin, we found more synergistic combinations between these macrolides and other tested drugs. Both azithromycin and clarithromycin are strongly synergistic with linezolid (log_2FIC_{50} of -1.1 and -0.99, respectively), an oxazolidinone that is suggested to treat *M. abscessus*. Azithromycin

and clarithromycin are also synergistic with cell-wall-acting drugs (except with cerulenin), RNA polymerase inhibitors, and respiratory inhibitors (Fig. 2A). These data suggest that there is potential to improve treatment outcomes by combining these core bacteriostatic protein elongation inhibitors with antibiotics that disrupt initiation of protein synthesis (linezolid) or target other cellular processes.

Clinically used antibiotics and other common antituberculosis agents: Besides amikacin and macrolides, other drugs recommended for treating *M. abscessus* are imipenem, cefoxitin, tigecycline, clofazimine, and linezolid (12). Among this list, we focused on linezolid and cefoxitin due to drug availability and reproducibility. **Linezolid:** We observed synergies between linezolid and some of the drugs used in the clinic, such as azithromycin and clarithromycin ($\log_2FIC_{50}$ of -1.1 and -1.0, respectively). Linezolid is strongly antagonistic with DNA-targeting antibiotics in our drug set while synergistic with cell-wall-acting drugs and respiratory inhibitors (Fig 2A), suggesting an underlying relationship between drug interaction and mechanism of action. We did not observe a synergistic relationship between linezolid and amikacin, which was previously reported in another study (28). However, there are several differences between the two studies that may account for these differences, including the media used (7H9 medium with supplements vs. CAMHB), strains (ATCC19977 vs. clinical isolates from patients), and method used to determine drug interaction (DiaMOND vs. broth microdilution). **Cefoxitin:** Cefoxitin is one of the few ß-lactams recommended to treat *M. abscessus*, besides imipenem (31). We could not obtain a reliable dose-response curve for both imipenem and cefoxitin, which may be due to the instability of ß-lactams in solution or the presence of the bla_{mab} gene that confers their resistance to ß-lactam. Nevertheless, one combination that passed our quality control is bedaquiline and cefoxitin ($\log_2FIC_{50}$ of 0.25). The antagonistic relationship between bedaquiline and cefoxitin has been reported in another study (32). It is thought that cefoxitin (and imipenem) triggers an ATP burst in *M. abscessus* by increasing oxidative phosphorylation, which is suppressed by bedaquiline, an F-ATP synthase inhibitor, leading to an elimination of the bactericidal effect of cefoxitin against *M. abscessus* (32, 33). Though this result is preliminary, it suggests that combining ß-lactams with bedaquiline could be unfavorable. **Moxifloxacin:** Moxifloxacin and other fluoroquinolones have been shown to have good activities against *M. abscessus* isolates *in vivo* (34). We and others have observed that moxifloxacin is antagonistic with azithromycin *in vitro* ($\log_2FIC_{50}$ of 0.23) and *in vivo* (35). We also observed that moxifloxacin is antagonistic with recommended antibiotics such

as amikacin and linezolid (log_2FIC_{50} of 0.31 and 0.68 respectively), suggesting its inclusion in multidrug therapies should be carefully considered. **Ethambutol:** Ethambutol is another antituberculosis agent with potential activity against NTMs such as *Mycobacterium avium* complex (MAC) due to its ability to slow the acquisition of macrolide-resistance clinically (36). The interactions of ethambutol with other drugs used to treat NTMs are unknown. Here, we observed a synergistic relationship of ethambutol with linezolid or azithromycin but not amikacin (log_2FIC_{50} of -0.79, -0.28 and 0.4 respectively), suggesting potential for exploring of ethambutol for *M. abscessus* treatment. **Rifampicin:** Rifamycin is a common antituberculosis agent that is highly potent *in vivo* and reduces relapse rate in combination therapies (37). However, rifampicin is not commonly used for *M. abscessus* because they are known to be intrinsically resistant to rifampicin (38). *M. abscessus* resistance to rifampicin partially due to its intrinsically low cell-wall permeability, possibly due to high lipid content, as well as drug efflux pump (37, 39). Additionally, *M. abscessus* encodes rifampicin ADP-ribosyltransferase (Arr_{Mab}), whose function is to catalyze ADP-ribosylation and render rifampicin inactive (40, 41). Though rifampicin does not have high potency against *M. abscessus*, our dataset demostrate synergistic interaction between rifampicin with many tested drugs, including amikacin and azithromycin. Rifampicin also synergizes all cell-wall-acting antibiotics in our dataset; the mechanism of synergy may be due to a weakened cell wall allowing better entry for rifampicin. Though rifabutin, another rifamycin antibiotic, has been approved to treat Mycobacterium Avium Complex and TB, its potential against *M. abscessus* has not been fully explored. Recent findings demonstrate limited modification of rifabutin by the Arr_{Mab} in comparison to rifampicin, resulting in lower MICs against both the ATCC19977 strain and clinical *M. abscessus* isolates (42). We also observed in our dataset that rifabutin has a lower IC_{50} and is more potent than rifampicin (IC_{50} of 1.8µg/mL versus 16 µg/mL, respectively, Table 1, Fig. 4A). However, rifabutin in our pairwise combinations tend toward antagonism, indicated by more red squares in the heat map compared to rifampicin (Fig. 2A). Nevertheless, rifabutin remains synergistic with frontline *M. abscessus* antibiotics such as clarithromycin (which has also been reported by other study), amikacin, and azithromycin, suggesting that rifabutin may be part of a clinically useful combination therapy (43). The rifamycin pairwise interaction data support continued exploration of this important class of drugs for treatment of *M. abscessus* infections.

Non-traditional NTM antibiotics

Next, we evaluated an unexplored space in combination therapies by analyzing drug interactions among antibacterials that are not traditionally used to treat NTMs and TB. **Telithromycin:** Telithromycin belongs to a large group of ketolides, a newer generation of macrolide with a slightly different mechanism of action (44, 45). Ketolides appear to partially inhibit protein synthesis rather than complete or near-complete inhibition of protein synthesis, which leads to more cellular degradation and a stronger bactericidal effect (45, 46). Despite being designed to be an alternative for some macrolide-resistant bacteria, telithromycin is not often used in the clinic due to its toxic side effects on the liver (47). We observed particularly strong synergies between telithromycin and other antibacterial compounds such as nitrofurantoin, rifampicin, amoxicillin, thioridazine, and azithromycin (log_2FIC_{50} of -1.7, -1.7, -2.7, -2.4, and -0.76, respectively), suggesting the potential of using combinations containing telithromycin to treat macrolide-resistant *M. abscessus*. Nevertheless, telithromycin is mildly antagonistic with amikacin and additive with linezolid (log_2FIC_{50} of 0.09 and -0.02, respectively). Therefore, further evaluation may be required before combining telithromycin with these clinically recommended drugs. **Amoxicillin and vancomycin:** Cell-wall-acting antibiotics amoxicillin and vancomycin show broad synergies with different classes of antimycobacterial (Fig. 2A). We found that amoxicillin is synergistic with almost all the tested partner drugs, including amikacin, azithromycin, clarithromycin, rifampicin, and ethambutol (log_2FIC_{50} of -0.58, -0.94, -0.87, -1.2, and -1.2, respectively). Amoxicillin has previously been known to enhance the effect of ß-lactam antibiotics such as imipenem and relebactam (48). Our results suggest that amoxicillin may also partner well with a broad range of antibiotics. For example, amoxicillin and telithromycin are strongly synergistic, with a log_2FIC_{50} of -2.7 (the most synergistic combo in our dataset). Vancomycin is another widely synergistic drug in our drug panel and was reported to be synergistic with clarithromycin, one of the most used clinical drugs for *M. abscessus* (49). Although we did not obtain a reliable drug interaction measurement for vancomycin with clarithromycin due to poor reproducibility, vancomycin is a promising candidate for a multi-drug regimen which showed broad synergy with most of the other drugs tested, except with thioridazine (Fig. 2A). Together, these data suggest that telithromycin, vancomycin, and amoxicillin, despite being uncommon drugs to choose in the clinic, tend toward synergy and may be candidates as partner drugs for *M. abscesses* regimen development.

Bedaquiline

Another drug candidate for the combination treatment of *M. abscessus* is bedaquiline, a diarylquinoline that inhibits subunit c of mycobacterial ATP synthase. In a zebrafish model of *M. abscessus* infection, bedaquiline was shown to exert a therapeutic effect by preventing the formation of abscesses (50). Additionally, a preliminary study in the clinic demonstrated the efficacy of using bedaquiline as salvage therapy. Within three months of treatment, bedaquiline reduced the bacterial load in the sputum of patients (51). Consistent with this finding, we found bedaquiline to have a low IC_{50} value of 0.16 µg/mL (Table 1). With DiaMOND, we observe that bedaquiline mildly antagonizes cefoxitin and amoxicillin (log_2FIC_{50} of 0.25 and 0.14, respectively) and is mildly synergistic with vancomycin and ethambutol (log_2FIC_{50} of -0.35 and -0.08. respectively). The antagonistic relationship between bedaquiline and cefoxitin in our data set is in agreement with previous studies that suggested bedaquiline eliminates the effects of ß-lactams (52). To evaluate the potential of bedaquiline more fully, we investigated drug interactions between bedaquiline and other antibiotics where these drug interactions have not yet been reported. We observed an overall trend that bedaquiline is antagonistic with DNA-acting antibiotics used in this study (Fig. 2A). In contrast, bedaquiline is synergistic with protein synthesis targeting drugs and thioridazine (Fig. 2A). Bedaquiline's potency and synergy with clinically favored protein synthesis inhibitors, such as amikacin and azithromycin (log_2FIC_{50} of -0.42 and -0.35, respectively) have not been previously reported to our knowledge. However, the administration of bedaquiline following amikacin yields positive clinical outcomes and has been reported for macrolide-resistant *M. fortuitum* complex soft tissue infection (53). A small preliminary report also suggested the potential clinical and microbiologic activity of bedaquiline against *M. abscessus* (51). Though current clinical results on bedaquiline are limited and further studies are required, these results suggested that bedaquiline should be explored for treating *M. abscessus*, and combinations containing bedaquiline could be considered for macrolide-resistant cases.

Thioridazine is an atypical antipsychotic still available in generic form, but with limited clinical use because of QTc prolongation (54). This agent initially gained interest for its potential use in treatment of MDR-Tb, as it has been shown to have properties against Mtb *in vitro*, *in vivo*, and in clinical cases, irrespective of antibiotic resistance status (55). In this study, thioridazine is synergistic with clinically preferred drugs such as amikacin, azithromycin, and clarithromycin (log_2FIC_{50} of -0.04, -0.46, and -0.22, respectively), as well as drugs that are not traditionally used for NTM treatment such as telithromycin, and

bedaquiline (log_2FIC_{50} of -2.4 and -0.72, respectively). Although thioridazine does not appear to have a strongly synergistic drug interaction profile (Fig. 2A), it is one of a few drugs in this dataset that shows synergy with clinically preferred drugs (other drugs are bedaquiline, vancomycin, and amoxicillin), suggesting that non-traditional antibiotics such as thioridazine could be useful in combination with other agents for *M. abscessus* infection, where the intrinsic resistance to common antibiotics is a challenge for treatment success.

SPR719

Another promising candidate for *M. abscessus* multi-drug regimen development is SPR719. SPR719 is a DNA gyrase inhibitor (GyrB) that is currently in clinical studies as a treatment for NTM infections, and is the prodrug version of SPR720, which is in phase I clinical development as a new oral agent for NTM infection and Mtb infection (56). We determined the IC_{50} of SPR719 to be 0.39 µg/mL **(**Table 1**)**, in agreement with the reported IC_{50} from previous studies (0.25 – 4 µg/mL, (26)). Despite being highly potent, the interaction profile of SPR719 is relatively mild, with a balanced profile of synergies and antagonisms (an even number of synergistic combinations, having $log_2FIC_{50} < 0$ and antagonistic combinations $log_2FIC_{50} > 0$ (Fig. 2A)). SPR719 is additive with amikacin (log_2FIC_{50} of -0.09) and synergistic with drugs from a broad range of classes used to treat NTMs and TB, including azithromycin, telithromycin, rifampicin (log_2FIC_{50} of -0.49, -0.26 and -0.19, respectively), and all cell-wall acting antibiotics tested (Fig. 2A). Through genomic analysis, *M. abscessus* was shown to contain a natural A92S mutation in *gyrB*, which is unique among other NTMs and *M. tuberculosis* (57). This mutation causes a conformational change in the ATP binding site, which may partially explain the intrinsic resistance of NTMs to GyrB inhibitors (57, 58). Despite this mutation, SPR719 is still very potent against *M. abscessus* (Table 1, Fig. 4A) (58). SPR719 is more potent than the fluoroquinolone moxifloxacin and is synergistic with more combinations compared to moxifloxacin (moxifloxacin log_2FIC_{50} median is 0.22 with only four combinations having $log_2FIC_{50} < 0$) (Table 1, Fig. 4A). Although moxifloxacin is not commonly recommended to treat *M. abscessus*, moxifloxacin is still being used in conjunction with amikacin and macrolides in clinical settings (12, 59). Together, these data suggest that SPR719 may be part of improved combination therapies for *M. abscessus*, including as a replacement for moxifloxacin.

Antibiotic potentiation to improve combinations therapy against *M. abscessus*

To determine whether a potentiator candidate enhances or attenuates the potency of antibiotics, we measured how the addition of potentiator candidates shifts the partner antibiotic's dose-response curve (Fig. 1B-C, Fig. 3A). We quantified the degree of potentiation (and attenuation) by calculating the $\log_2$-transformed fold shift in IC_{50} or IC_{90} of the effective antibiotic with the addition of a constant dose of the candidate potentiator so that a negative $\log_2$FsIC indicates potentiation and a positive value indications attenuation (Fig. 1B-C). We observed that all tested antibiotics were attenuated by all four potentiator candidates at IC_{50}, but some antibiotics were potentiated at IC_{90} (Fig. 3A). For example, avibactam attenuates the effect of amikacin at IC_{50}, indicated by the right shift in combination dose-response curves compared to the amikacin dose-response curve ($\log_2$FsIC_{50} of 1.1, Fig. 3B). However, with avibactam, amikacin reached IC_{90} at a lower concentration, indicated by a left shift in the combination dose-response curve compared to single-drug dose-response curve ($\log_2$FsIC_{90} of -2.1, Fig. 3B), indicating a potentiating effect. We observe a similar shift in all combinations where IC_{90} is reported, e.g., potentiator candidates shifted from being attenuating to either less attenuating (such as bedaquiline with streptomycin; $\log_2$FsIC shifts from 6.4 at IC_{50} to 4.2 at IC_{90}), or from attenuating to potentiating (as with the previous example between amikacin and avibactam), or from less potentiating to more potentiating (such as avibactam and rifabutin; $\log_2$FsIC shift from 0.04 at IC_{50} to -3.4 at IC_{90}, Fig. 3B). This dramatic shift from attenuation to potentiation is explained by an increase in the steepness of the dose-response curve with the addition of potentiator candidates so that the effect in some combinations is an increase in potency at higher dose levels of the antibiotic (Fig. 3B). Among four tested potentiator candidates, streptomycin has the strongest attenuating effect at IC_{50} and IC_{90} (except with rifabutin and levofloxacin, in which case streptomycin acts as a potentiator). Among our tested drug set, three inactive drugs potentiate the activity of rifabutin (with the 4^{th} being unmeasurable).

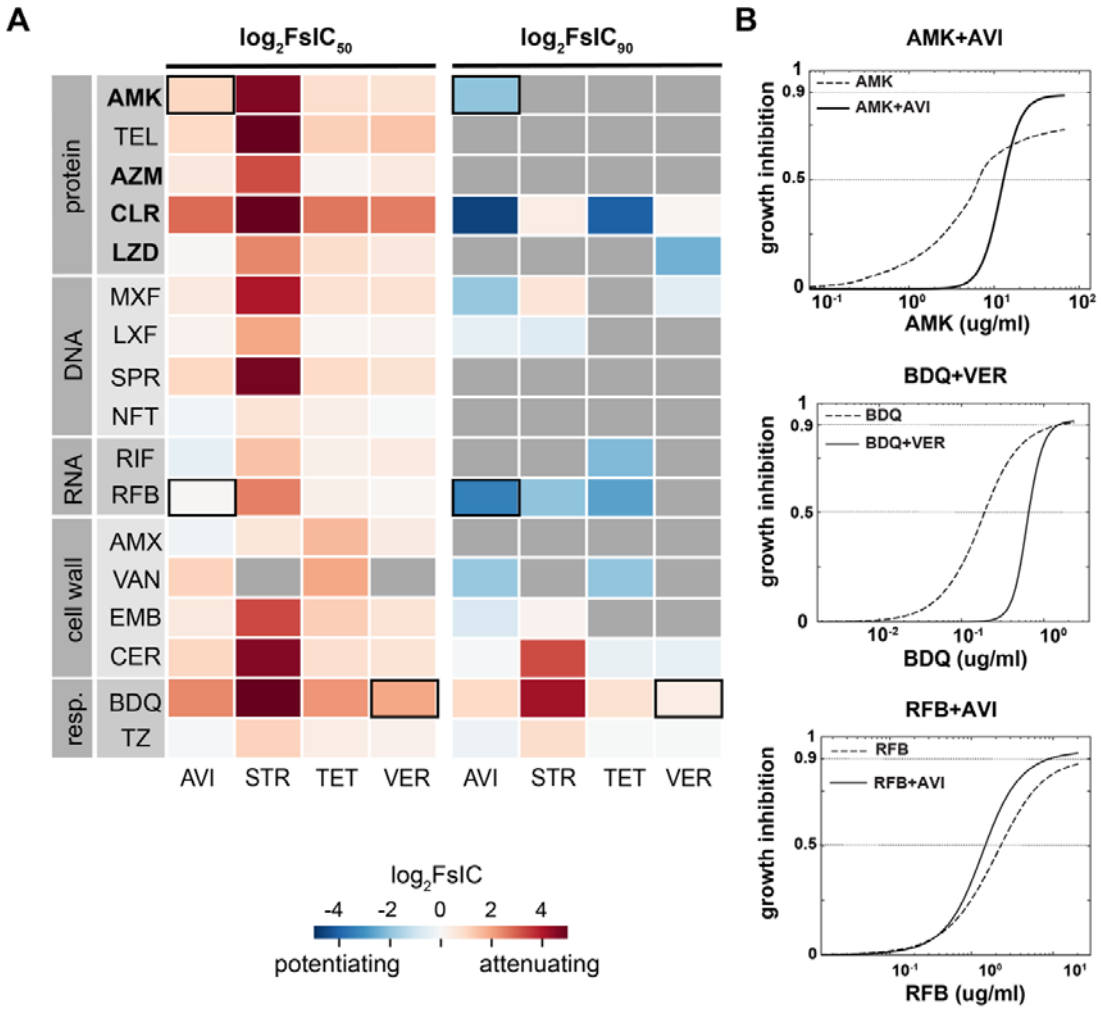

FIG 3. Effect of potentiator candidates on antibiotic efficacies in *M. abscessus* ATCC19977. (A) Heat map of pairwise drug interactions with potentiators at a fixed concentration. Drugs are categorized based on their mechanism of action and drugs recommended for treating *M. abscessus* infection are indicated in bold text. Drug interaction measurement is expressed as the change in log2 fold shift at IC_{50} (left) or IC_{90} (right). $Log_2FsIC < 0$ indicates potentiating effects, shown in blue, and $log_2FsIC > 0$ indicate attenuating effects, shown in red. Outline squares indicate combinations that are shown in the dose-response below. (B) Example dose-response curves showing the fold shift in IC_{50} and IC_{90} for drugs combined with potentiators, amikacin (AMK) + avibactam (AVI) (top), bedaquiline (BDQ) + verapamil (VER) (middle), rifabutin (RFB) + avibactam (AVI) (bottom). The dash line indicates the single drug dose-response curve, while the solid line represents the combination curve. A left shift in the solid line dose-response curve indicates a potentiating effect, and a right shift shows an attenuated effect by the potentiator.

Beta-lactams are the most widely used antibiotics (60). However, due to the presence of the broad-spectrum beta-lactamase Bla_{Mab}, only imipenem and cefoxitin are currently recommended in the multidrug-regimens targeting *M. abscessus* (8). Therefore, potentiators such as avibactam, a non-ß-lactam ß-lactamase inhibitor shown to efficiently inhibit Bla_{Mab}, can potentially help extend the spectrum of ß-lactam antibiotics active against *M. abscessus* (61). Porins of *M. abscessus* cell wall have been shown to partially contribute to ß-lactam resistance as they allow hydrophilic molecules to cross the cell membrane, which can interact with the target in the cytoplasm and potentially trigger the expression of resistance genes (10, 62). Avibactam has also been reported to reduce the MIC of cell-wall-acting agents (63), and we observed a potentiating effect of avibactam with cell-wall-acting agents ethambutol, cerulenin, and vancomycin (log_2FsIC_{90} of -0.76, -0.072, and -1.9) at IC_{90}. Because avibactam is a ß-lactamase inhibitor, we also wanted to determine its effect with amoxicillin. Due to the low potency of amoxicillin, there is no IC_{90} for amoxicillin. However, at IC_{50}, we observed a mild potentiating effect (log_2FsIC_{50} of -0.2), which is not commonly observed in our dataset (the other combinations are avibactam and nitrofurantoin, log_2FsIC_{50} of -0.2, avibactam and rifampicin, log_2FsIC_{50} of -0.44, and avibactam with thioridazine, log_2FsIC_{50} of -0.061).

Although verapamil is not effective on its own and have limited clinical used due to its primary effect on cardiac function, verapamil at 50 µg/mL was reported to enhance the killing of bedaquiline in *M. abscessus* (23, 64). In contrast, our data show a right shift (attenuation) of the bedaquiline + verapamil dose-response curve compared to the bedaquiline single dose-response curve (log_2FsIC_{50} value of 1.9, Fig. 3B). This difference in the role of verapamil on bedaquiline efficacy may be due to experimental differences such as verapamil concentration. In Viljoen et al., 50µg/mL of verapamil was used, whereas we used a lower dose of 2.35 µg/mL, which was chosen based on 3-fold maximum plasma concentration 4-6 hours after administration, assuming one pill of 100 mg of bedaquiline was administered (65).

We observed that streptomycin and verapamil largely attenuated the potency of partner drugs, whereas avibactam and tetracycline are broadly potentiating at IC_{90} (Fig. 3A), suggesting that these two candidates should be further explored as an element of multi-drug treatment for *M. abscessus* infection. Additionally, we showed that with modification, DiaMOND can be used to measure the combined effect between a potentiator and an active drug.

Drug interactions cannot be predicted from single drug potencies or mechanisms of action

In the absence of a known effective multidrug therapy for *M. abscessus* infection, clinicians usually rely on single drug susceptibility profiles and their own experience to determine the best drug combination for each patient. In some cancers, single-drug susceptibility profiles can be used to design optimized combination therapies under the principle that efficacy for each cancer is determined by its susceptibility to any of the agents and that combination therapies were effective as bet-hedging strategies (66). To understand whether we could predict drug interactions based on single-drug properties, we started by evaluating whether single-drug potencies were correlated with the propensity for drug interactions to be synergistic or antagonistic in *M. abscessus*. In Fig 4A, single drugs are organized based on their IC_{50} on the x-axis, and the y-axis shows the distribution of $\log_2FIC_{50}$ of all combinations containing that single drug. We do not observe a correlation between distributions of $\log_2FIC_{50}$ compared to IC_{50} for each drug, suggesting that drug interactions cannot be predicted from single drug potencies. We wondered if the most potent or least potent antibiotic is the driver of drug interaction, which may be obscured by looking at the overall propensity for synergy compared to single-drug potencies. To take the IC_{50} of both drugs in each pairwise combination into consideration, we evaluated whether there were patterns of synergy and antagonism compared to the IC_{50}s of both partner drugs (Fig. 4B). In the drug interactions among 18 antibiotics, there was no clear trend of synergy and antagonism based on single-drug potencies (e.g., the drug interactions, colored by $\log_2FIC_{50}$, are not clustered by drug potency to either drug). For example, SPR719 and bedaquiline are highly potent drugs with low IC_{50} (IC_{50} of 0.39 µg/mL and 0.16 µg/mL, respectively), but the combination between SPR719 and bedaquiline are antagonistic ($\log_2FIC_{50}$ of 0.74). Conversely, amikacin and amoxicillin are not as potent as SPR719 or bedaquiline (IC_{50} of 6.6 µg/mL and 300 µg/mL, respectively) but are mildly synergistic in combination ($\log_2FIC_{50}$ of -0.59). Together, our analysis demonstrates that single drug potency is not predictive of drug interactions, and we cannot anticipate whether a drug pair will be synergistic or antagonistic based on their potency profiles as single agents.

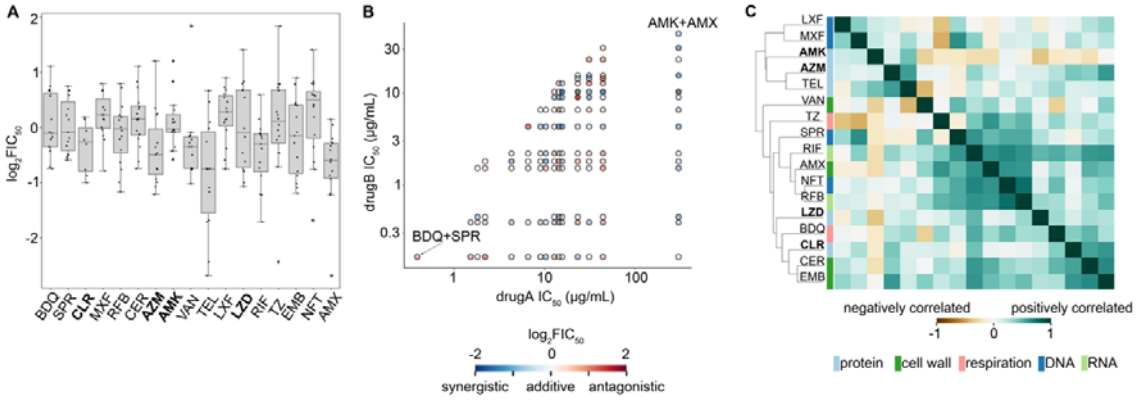

FIG 4. Relationship between drug potency or mechanism of action with synergy (A) Box plot of drug interaction (log_2FIC_{50}) of all combinations containing the single drug represented on the x-axis, drugs recommended for treating *M. abscessus* infection are indicated in bold text. Each dot inside the box represents a combination of that single drug and another drug in the data set. Single drugs are ordered on the x-axis based on IC_{50} (Table 1), with drugs having the highest IC_{50} on the right and the lowest IC_{50} on the left (B) Comparison of drug interaction scores with single drug potency in ATCC1977. Pairwise combinations are plotted as the components of their single drug IC_{50} (μg/mL). Given a pairwise combination, the potency of a single drug is plotted on the y-axis while the non-potent drug is on the x-axis; drugs recommended for treating *M. abscessus* infection are indicated in bold text. The color fill indicates the synergistic (blue) or antagonistic (red) interaction in ATCC19977. (C) Clustering of drugs' interaction profile in ATCC19977. Each box represents the Pearson correlation of drug interaction profiles between two antibiotics. 1 indicates a positive correlation, whereas -1 indicates a negative correlation. The color bar along the y-axis represents the general drug target pathway (e.g., inhibition of protein, cell wall, DNA, or RNA synthesis and inhibition of respiration.)

Next, we evaluated whether there were drug interaction patterns that correspond to each partner drug's mechanism of action. To test the hypothesis that drugs targeting similar pathways would have similar interaction profiles, we compared the similarities among drug interaction profiles from the 17 antibiotics that target four general processes using hierarchical clustering (Fig. 4C). Cefoxitin is removed from this analysis because there is only one reportable combination containing cefoxitin in our dataset. In general, it is unclear whether drug interaction profiles are clustered by the mechanism of action. For example, rifabutin and nitrofurantoin have similar interaction profiles but different mechanisms of

action. However, there are also examples of drugs with a similar mechanism of action that have similar interaction profiles, such as cell-wall acting agents ethambutol and cerulenin, the fluoroquinolones levofloxacin and moxifloxacin, protein synthesis inhibitors azithromycin and telithromycin (Fig. 4C). Nevertheless, it is possible that an analysis of drug interaction profiles across a larger set of drugs may reveal patterns that are not present in this dataset due to the small number of representatives for each drug class. Further analysis with a larger drug set with an even greater number of representatives for each drug category may be necessary to understand whether drug interaction patterns are similar in *M. abscessus* for drugs with closely related mechanisms of action. However, our data do not suggest that there are strong similarities in drug interactions for drugs that target the same pathways.

Drug interaction is strain-specific

An extensive study of 85 clinical isolates from *M. abscessus* subspecies demonstrated species-specific drug susceptibility, including clinically favored drugs, such as amikacin and macrolide clarithromycin (67). For this reason, we speculated that drug interactions would also vary from isolate to isolate. To test this hypothesis, we selected three strains that were chosen to represent major types of variation among strains, including colony morphology (e.g., smooth versus rough phenotype) and growth rate (e.g., slow- versus fast-growing). The fastest and the slowest growing strain were the lab reference strain ATCC19977 and TMC2 (4hr and 20hr doubling, respectively, Table S2). ATCC19977 and TMC3 shared similar smooth morphologies, and TMC1 and TMC2 shared similar rough morphologies. Detailed information about the doubling time and phenotype of these clinical isolates is included in Table S2.

We used a focused drug set for isolate-to-isolate comparison; the set includes antibiotics that are recommended for current therapies for NTMs and TB (amikacin, azithromycin, cefoxitin, clarithromycin, moxifloxacin, and rifampicin), in development (SPR719 and bedaquiline), or are broadly synergistic in ATCC19977 (telithromycin). Consistent with previous studies, we observed variation in IC_{50} values from isolate-to-isolate (Fig. 5A) (11, 67). Though susceptibility among strains is also variable for newer drugs, some relative potencies for single-antibiotics are retained across strains. For example, bedaquiline and SPR719 have the highest potency (e.g., lowest IC_{50}) for the lab reference strain, and this observation holds for other strains (except for SPR719 in TMC3 strains, Fig. 5A). To understand if colony morphotype or growth rate was correlated with drug susceptibility, we calculated Pearson correlations of IC_{50} values between each strain (Fig. S4A). In general, we observed poor

599 correlations in single-drug susceptibility patterns between strains, even in strains with
600 common morphologies and similar growth rates (ATCC1977, TMC3) and (Table 2, Fig.
601 S4A). The only significant correlation (R = 0.88) observed is between TMC2 and
602 ATCC19977, which differ in both morphology and growth rate **(**Table 2). Together, our data
603 suggest that isolate-to-isolate differences in drug response are not well correlated with colony
604 morphology and doubling times.

605 **Table 2. Characterization of lab strain (ATCC19977) and clinical isolates TMC1, TMC2**
606 **and TMC3**

strain	doubling time (hour)	morphology
ATCC19977	4	smooth
TMC 1	12	rough
TMC 2	20	rough
TMC 3	8	smooth

607

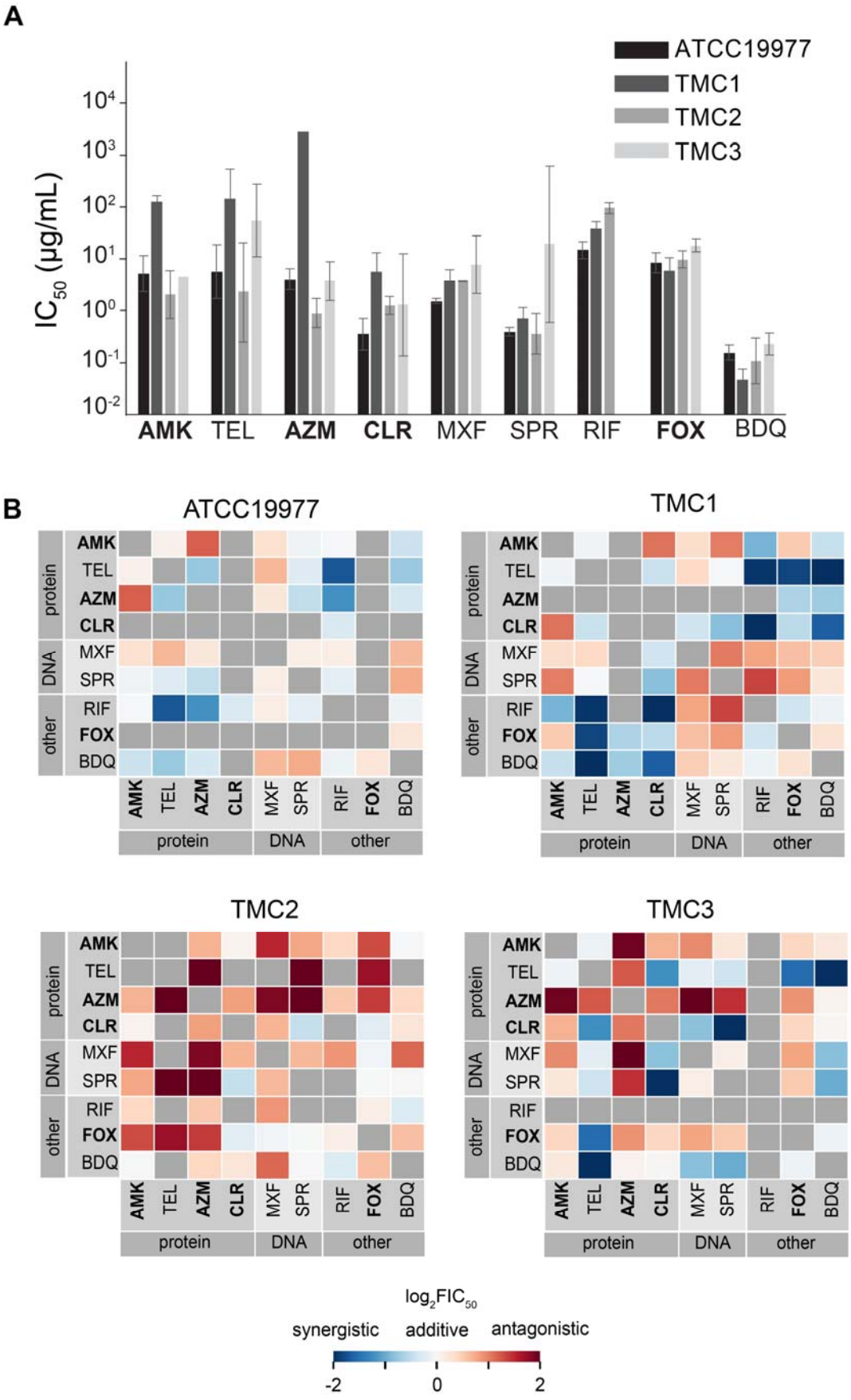

608

FIG 5. Single drug susceptibility and drug interaction outcomes and in different *M. abscessus* clinical isolates. (A) Single drug susceptibilities for the reference strain (ATCC19977) and three clinical isolates (TMC1, TMC2, and TMC3). Susceptibility is measured by the IC_{50} (μg/ml). Error bars represent standard deviation as compared to the mean, when there are more than one replicates IC values are reported. (B) Heat map showing drug interactions for each strain: ATCC19977 (top left), TMC1 (top right), TMC2 (bottom left) and TMC3 (bottom right). As in Fig 2, drugs are organized by the mechanism of action, and drugs recommended for treating *M. abscessus* infection are indicated in bold text. Drug measurement is expressed in $\log_2 FIC_{50}$, where blue highlights $\log_2 FIC < 0$ (synergy) and red is $\log_2 FIC > 0$ (antagonism).

To understand whether drug interactions were also strain-dependent, we measured pairwise drug interactions among the nine drugs in our focused antibiotics set with DiaMOND. The drug interaction profiles varied from isolate to isolate (Fig. 5B). Correlation analysis demonstrates that the most similarity in drug interactions is between TMC1 and ATCC19977 (R = 0.48, Fig. S4B). We noted that there was no correlation in single-drug IC_{50} values between TMC1 and ATCC19977, nor did these two strains share morphologies or growth rates. The lack of similarity between these strains, except in the drug interaction profile, supports our hypothesis that drug interaction is independent of single drug potency and morphology. The spectrum of drug interactions is balanced in ATCC19977, TMC1, and TMC3, whereas TMC2 strongly tends toward antagonism **(**Fig. 5B). Despite poor overall correlations in drug interaction profiles from strain to strain, we observed some similarities between these strains. For example, amikacin paired with macrolides (such as azithromycin or clarithromycin) is consistently antagonistic. In contrast, combinations of clarithromycin and SPR719 or bedaquiline and telithromycin were all synergistic (Fig. 5B). There are strongly synergistic combinations such as clarithromycin with almost all tested drugs for TMC1 (except amikacin) or telithromycin with almost all tested drugs for TMC3 (except amikacin and azithromycin) (Fig. 5B), suggesting that there may be space for improvement in combination therapy in a strain specific manner. Taken together, our results affirm the need for targeted drug combination testing and suggest that measurements should be made for each isolate for reliable drug interaction determination.

DISCUSSION

Infections caused by *M. abscessus* are notoriously difficult to treat for many reasons, including innate and acquired drug resistance, low antibiotic efficacies, and variation among

strains. Combination antibiotic treatment has the potential to improve treatment efficacies via synergies and potentiation. Despite this potential and reports of several synergistic drug combinations, we have lacked a comprehensive drug interaction dataset to develop drug combinations for the treatment of *M. abscessus*. Here, we applied DiaMOND to systematically measure pairwise drug interactions among 18 drugs against *M. abscessus* to better understand the landscape and potential of combination therapy for effective treatment. Our results include 122 drug pairs for which we report interactions for the first time. These data revealed an unexpectedly large synergy space compared to other bacterial species. We observe many synergistic drug pairs that are currently not considered as options for treating *M. abscessus* pulmonary infection in clinical practice. One example is amoxicillin, which is not currently recommended to be used to treat *M. abscessus*. Amoxicillin is synergistic with almost all tested drugs, combined with its clinical practicality suggests its potential to be used in combination therapy. We did not find that clinically used drug pairs were necessarily synergistic *in vitro*. For example, amikacin and azithromycin is antagonistic *in vitro* while another pair of protein synthesis inhibitors (azithromycin and linezolid) is synergistic. Together, the large number of synergies identified here *in vitro* motivates future investigation of these combinations as a path forward to improve combination therapy to treat pulmonary *M. abscessus* infection.

Our findings demonstrate that some drugs that are not effective alone potentiate the activities of other antibiotics. These agents may play an important role in improving *M. abscessus* regimens given the poor efficacy of antibiotics as monotherapies for *M. abscessus*. To understand whether we could sensitize *M. abscessus* to antibiotics using potentiators, we expanded our combinations screen and adapted the DiaMOND methodology to evaluate how drugs that are considered inactive affect the efficacies of active drugs. Among the four candidate potentiators we tested, avibactam has been subjected to multiple studies due to its ability to inhibit Bla_{mab} and potentially allow more ß-lactams to be used to treat *M. abscessus*. Our results are consistent with previously reported studies on combining a non-ß-lactam ß-lactamase inhibitor with ß-lactam to extend the efficacy of ß-lactam, which suggests that avibactam should be considered in a multi-drug therapy (61, 63). Additionally, the most potentiating effect is observed at 90% growth inhibition (not 50% growth inhibition), suggesting that the potentiators' effect is likely to be more prominent at higher concentrations of the active antibiotic.

We found that we could not predict drug interactions based on drug potencies or mechanisms of action. Though drug interaction profiles were not very similar among antimicrobials targeting the same cellular process (cell wall, DNA, etc.), we observed that some antibiotics were consistently synergistic or antagonistic with drugs from the same class. For example, DNA-targeting drugs are antagonistic with linezolid and respiratory inhibitors (bedaquiline and thioridazine) and synergistic with cell-wall-acting antibiotics (ethambutol, vancomycin, and amoxicillin). The reason for the observed synergy between cell-wall-acting and DNA-acting compounds may be due to cell wall targeting compounds increasing the permeability of the mycobacterial cell wall, resulting in an increased accumulation of DNA-targeting compounds in the cell (68). *M. abscessus* is known to increase the activity of efflux pump inhibitors when exposed to bedaquiline, which may result in the rapid efflux of DNA-acting compounds and an antagonist interaction (23).

Another challenge with developing an effective regimen for *M. abscessus* is the remarkable variation in drug response among strains, likely due to genomic diversity in NTM species, even across morphologically related isolates (26, 69). We measured drug interactions in three clinical isolates with different colony morphologies and growth rates. Previous studies have shown that the impact of colony morphotype, which includes the transition of the smooth colony to the rough colony during infection, highly affects drug susceptibility (70). To understand whether a universal multidrug regimen may be developed that is effective against all *M. abscessus* strains, we measured a core set of drug pairs in different clinical strains of *M. abscessus*. We found that drug interactions were poorly correlated across strains and could not be systematically determined based on data from the reference strain, strains with similar morphologies or growth rates, the single-drug susceptibility profiles, or the drug mechanisms of action. This result suggests the potential need to include susceptibility testing for drug combinations, instead of single drugs only in clinical laboratory testing. Strain-to-strain variation in drug interaction profile may be determined by subspecies or genetic differences, for instance the presence of the *erm* gene, which can confer macrolide resistance. Future work measuring drug interactions across a large set of clinical isolates is required to address this question. Nevertheless, our observations drug interactions in *M. abscessus* are strain-specific supports the idea that treatment regimen development may need to be personalized for each isolate (e.g., directly measured) rather than derived from guidelines based on other strains.

706 This systematic study of the drug combination landscape in *M. abscessus* suggests that we
707 require a more extensive phenotypic evaluation of drug interactions to develop improved
708 therapies. Additionally, the relationship between *in vitro* single drug susceptibility or
709 combination measurement and clinical outcome in *M. abscessus* has not yet been sufficiently
710 studied, and it is currently unclear whether synergy correlates with positive clinical outcomes
711 (71). This challenge in linking *in vitro* measurement to *in vivo* response is not unique to
712 NTMs and is well characterized in tuberculosis (72, 73). However, previous studies have
713 shown that measurement of the drug combination response across multiple growth conditions
714 that resemble the host's microenvironment is predictive of treatment shortening in Mtb (30,
715 74). Environmental nutrients have a critical effect on drug interaction in both *M. abscessus*
716 and Mtb, and antibiotic response is altered when grown in artificial cystic fibrosis sputum (30,
717 75, 76). We, therefore, expect that making drug interaction measurements in different host-
718 mimicking growth conditions and testing which of these growth environments predicts
719 treatment outcomes in preclinical animal models and in humans is a critical step in drug
720 combination design for *M. abscessus* and other NTMs. Together, the dependence of drug
721 interactions on strain and variation in drug response with strain and growth conditions
722 suggests that we have failed to identify a universal combination therapy that is effective for
723 *M. abscessus* not because good drug combinations do not exist, but rather because we need to
724 better understand how to tailor combination therapy to each infection.

725 **MATERIALS AND METHODS**

726 **Antimicrobials**

727 The antimicrobials agents used in this study (except for SPR719) were obtained from Sigma
728 Aldrich. SPR719 was a gift from Spero Therapeutics. Stock solutions were prepared in
729 DMSO or sterile water + 0.01% Triton X-100, depending on solubility, and stored in single-
730 use aliquots at -20˚C until used.

731 **Strain and culturing**

732 Measurement was made using *M. abscessus* subsp. *abscessus* strain ATCC19977 (reference
733 strain) and clinical isolates obtained from patient sputum at Tufts Medical Center, Infectious
734 Disease Clinic (TMC1, TMC2, and TMC3) (77). All strains were cultured in a 7H9 medium
735 supplemented with 0.05% Tween 80, 0.2% Glycerol, and 10% BBL Middlebrook ADC
736 enrichment. Cultures were started from frozen aliquots and allowed to grow to the mid-log
737 phase (OD_{600} between 0.4 - 0.6), shaking at 37˚C overnight. Cultures were then diluted once

to the lag phase (OD_{600} between 0.05 - 0.1) and allowed to grow to the mid-log phase before performing assays.

DiaMOND measurement

DiaMOND was used to measure drug interactions, as previously described for *Mycobacterium tuberculosis* (18). Details of DiaMOND can be obtained in Mycobacteria Protocol 4th, chapter 30th (78). Briefly, DiaMOND uses equipotent drug-combination dose-response curves to approximate the shape of checkerboard isoboles at the same level of growth inhibition. Minor adjustments (e.g., the dose-response curve is centered around 50% inhibitory concentration (IC_{50}) in contrast to 90% inhibitory concentration (IC_{90}) for *M. tuberculosis*, the modification of fractional inhibition concentration to fold shifts in inhibition concentration) were made to account for the rapid growth of *M. abscessus* and low drug potency relative to *M. tuberculosis*. Details of these adjustments are explained in subsequent sections.

Growth inhibition assay

Antibiotics tested were either dissolved in dimethyl sulfoxide (DMSO) or sterile water + 0.01% Triton X-100 and stored at -20˚C in single-use aliquots. Assays were performed in clear, flat bottom 384-well microplates. Drugs were dispensed using a digital drug dispenser (D300e Digital Dispenser, HP). Drug wells were randomized across plates to minimize plate position effects. Bacterial cultures were diluted to OD_{600} of 0.05 in fresh medium, and 50µL of diluted culture was added to each well for drug treatment. Plates were sealed with optically clear plate seals and incubated without shaking at 37˚C. Growth (OD_{600}) was measured by a microplate reader (BioTek) 48h after drug treatment.

Data analysis

OD_{600} data were processed using MATLAB's custom analysis pipeline (MathWorks). Data were first derandomized from the plate layout, and dose-response curves were organized for each drug and drug combination. The first row of wells in each 384-well plate contained medium-only wells. The median of these medium-only wells was subtracted from each well in a plate as a background. Drug-treated wells were normalized to the mean of the untreated wells (controls), and the values obtained were subtracted from 1 to get a dose-response inhibition curve where 0 and 1 represented no growth inhibition and full growth inhibition, respectively. Growth inhibition curves were then fit to a three-parameter Hill curve using a nonlinear solver in MATLAB (79). The fit accuracy was assessed using the R^2 metric.

Equations derived from the Hill function were used to calculate different inhibitory concentration values (IC values) along the dose-response curve.

Drug interaction calculation

To assess whether drugs in combination were synergistic, additive, or antagonistic, we measured the fractional inhibitory concentrations (FIC). We used Loewe additivity as the null model to calculate the FIC values (80). We calculated the expected IC value of the combination AB (drug A with drug B) from the intersection of the combination line to the line of additivity determined by the IC values of A and B alone (Fig. 1A). Finally, the FIC value is calculated by dividing the experimentally observed IC by the expected IC value of the drug combination.

$$FIC = \frac{observed\ IC}{expected\ IC}$$

We report the $\log_2$ of the FIC so that the magnitude of synergy and antagonism scores are balanced around zero. A $\log_2$FIC value < 0 is synergistic, $\log_2$FIC value ~= 0 is additive, and $\log_2$FIC value > 0 is antagonistic. FIC scores were calculated at IC_{50} (FIC_{50}) and IC_{90} (FIC_{90}). With DiaMOND, we can measure drug interaction scores using other null models such as Bliss independence. By Bliss independence, the expected IC value for [AB] is calculated by multiplying drug A's effect and drug B's effect at the desired IC level.

Certain drugs were tested at a fixed concentration (instead of increasing doses) due to their lack of inhibitory effect as a single agent. These drugs are also referred to as potentiator candidates. The concentration of the potentiator candidates was estimated from previously reported serum concentrations. To quantify drug interaction scores for potentiators, fold shifts in ICs (FsICs) were calculated as a ratio of the observed IC_{50} value of a drug pair combination to the IC_{50} of the active, non-potentiating drug (Fig. 1B). Log_2FsIC < 0 are potentiated whereas $\log_2$FsIC > 0 are attenuated.

Quality control

Assay quality was assessed in three different ways. The Z-factor was used to determine the quality of the assay at the plate level. For a given plate, the Z-factor was calculated as:

$$Z' = 1 - \frac{3(\sigma_{positive} + \sigma_{negative})}{|\mu_{positive} - \mu_{negative}|}$$

where σ is the standard deviation of the positive and negative control (untreated cells), μ is the mean of the positive and negative controls. Plates with a Z' between 0.5 - 1 indicate excellent assay with a statistically reliable separation between positive and negative control.

The second level of assessment was at the dose-response level. The R^2 value derived from fits of the dose-response curves to Hill curves was used to determine fit accuracy. We combined R^2 values with a visual inspection of the fits. Any Hill curve fits with R^2 values below 0.7 were marked as poor fits and rejected from further analysis. Because of the intrinsic resistance property of *M. abscessus*, it is challenging to obtain consistent dose-response curves (81). For example, to capture data points close enough to each other to draw an accurate dose response, we need to design doses to increase by 1.5x instead of 2c, which limits the testing range. In addition, the noise of the dose-response curve made fitting challenging. Finally, obtaining a maximum inhibitory concentration (MIC) for all drugs is difficult due to the heterogeneity of *M. abscessus* (81). To overcome these difficulties, we designed the experiment around IC_{50} (instead of IC_{90}), which is achieved for most drugs and is more reproducible than IC_{90} (Table S1). To assess whether doses were sampled in an equipotent manner for combination dose-response, the angle of the combination dose-response was calculated (the ideal angle is 45˚). Angle deviation beyond 22.5˚ of this ideal equipotent dose-response was deemed too far for the approximation of isoboles in the checkerboard and was eliminated from the analysis.

Clinical isolate growth rate measurement

To measure the growth rate of clinical isolates obtained from patient sputum at the Tufts Medical Center Infectious Disease Clinic (TMC1, TMC2, and TMC3), suspended culture of these isolates were grown in a 7H9 medium supplemented with 0.05% Tween 80, 0.2% Glycerol, and 10% BBL Middlebrook ADC enrichment. Cultures were started from frozen aliquots and allowed to grow to the mid-log phase (OD_{600} between 0.4 - 0.6), shaking at 37˚C overnight. Cultures were then diluted once to the lag phase and allowed to grow to the mid-log phase again before performing the assay. Growth rate measurement was performed in a 96-well microplate, with five biological replicates per isolate. Reference strain ATCC19977 was also included for reference purposes. 150µL of culture at OD_{600} around 0.05 was dispensed into each well. The microplate was sealed with an optically clear plate seal and incubated inside a plate reader at 37˚C. OD_{600} was recorded for 18 hours in 30 minutes intervals. Doubling time was calculated using OD_{600} values closest to the log phase. Doubling time was calculated as:

$$r = \frac{\ln\left(OD'_{600} - OD_{600}\right)}{(T' - T)}$$

$$Doubling\ time = \frac{ln2}{r}$$

ACKNOWLEDGEMENTS

We thank members of the Aldridge laboratory, Veronique Dartois, Alyssa Greig, and Aisling Lavelle for insightful discussion. This work was supported in part by the Stuart B. Levy Center for Integrated Management of Antimicrobial Resistance at Tufts (Levy CIMAR), a collaboration of Tufts Medical Center and the Tufts University Office of the Vice Provost for Research Research and Scholarship Strategic Plan. BBA was supported, in part, by NIH 5R01AI150684 (to BBA). FPM was supported by a financial grant from Mukoviszidose Institut gGmbH, Bonn, the research and development arm of the German Cystic Fibrosis Association Mukoviszidose e.V (project number 2004 – FM). JK was supported by National Institution of General Medical Science (T32GM008448). PAL was supported by National Institution of General Medical Science (T32AI007422).

AUTHOR CONTRIBUTION

NV, YD, JLF, TS, and BBA conceived and designed the experiments. NV, YD, JK, and PL performed the experiments. NV, YD, and BBA conceived and designed the computational analysis. NV and YD performed the computational analysis. The manuscript was written by NV, YD, TS, and BBA. All authors contributed to the technical interpretation, interpretation of the results, and the editing of the manuscript.

REFERENCES

1. Minias A, Zukowska L, Lach J, Jagielski T, Strapagiel D, Kim SY, Koh WJ, Adam H, Bittner R, Truden S, Zolnir-Dovc M, Dziadek J. 2020. Subspecies-specific sequence detection for differentiation of Mycobacterium abscessus complex. Sci Rep 10:16415.

2. Ratnatunga CN, Lutzky VP, Kupz A, Doolan DL, Reid DW, Field M, Bell SC, Thomson RM, Miles JJ. 2020. The Rise of Non-Tuberculosis Mycobacterial Lung Disease. Front Immunol 11:303.

3. Quang NT, Jang J. 2021. Current Molecular Therapeutic Agents and Drug Candidates for Mycobacterium abscessus. Front Pharmacol 12:724725.

4. Wi YM. 2019. Treatment of Extrapulmonary Nontuberculous Mycobacterial Diseases. Infect Chemother 51:245-255.

5. Johansen MD, Herrmann JL, Kremer L. 2020. Non-tuberculous mycobacteria and the rise of Mycobacterium abscessus. Nat Rev Microbiol 18:392-407.

6. Maurer FP, Bruderer VL, Ritter C, Castelberg C, Bloemberg GV, Böttger EC. 2014. Lack of Antimicrobial Bactericidal Activity in Mycobacterium abscessus. Antimicrobial Agents and Chemotherapy 58:3828-3836.

7. Sander P, Rezwan M, Walker B, Rampini SK, Kroppenstedt RM, Ehlers S, Keller C, Keeble JR, Hagemeier M, Colston MJ, Springer B, Bottger EC. 2004. Lipoprotein processing is required for virulence of Mycobacterium tuberculosis. Mol Microbiol 52:1543-52.

8. Nessar R, Cambau E, Reyrat JM, Murray A, Gicquel B. 2012. Mycobacterium abscessus: a new antibiotic nightmare. J Antimicrob Chemother 67:810-8.

9. Pawlowski AC, Stogios PJ, Koteva K, Skarina T, Evdokimova E, Savchenko A, Wright GD. 2018. The evolution of substrate discrimination in macrolide antibiotic resistance enzymes. Nat Commun 9:112.

10. Nessar R, Cambau E, Reyrat JM, Murray A, Gicquel B. 2012. Mycobacterium abscessus: a new antibiotic nightmare. Journal of Antimicrobial Chemotherapy 67:810-818.

11. Weng Y-W, Huang C-K, Sy C-L, Wu K-S, Tsai H-C, Lee SS-J. 2020. Treatment for Mycobacterium abscessus complex–lung disease. Journal of the Formosan Medical Association 119:S58-S66.

12. Kurz SG, Zha BS, Herman DD, Holt MR, Daley CL, Ruminjo JK, Thomson CC. 2020. Summary for Clinicians: 2020 Clinical Practice Guideline Summary for the Treatment of Nontuberculous Mycobacterial Pulmonary Disease. Ann Am Thorac Soc 17:1033-1039.

13. Weng YW, Huang CK, Sy CL, Wu KS, Tsai HC, Lee SS. 2020. Treatment for Mycobacterium abscessus complex-lung disease. J Formos Med Assoc 119 Suppl 1:S58-S66.

14. Kwak N, Dalcolmo MP, Daley CL, Eather G, Gayoso R, Hasegawa N, Jhun BW, Koh W-J, Namkoong H, Park J, Thomson R, van Ingen J, Zweijpfenning SMH, Yim J-J.

2019. Mycobacterium abscessus pulmonary disease: individual patient data meta-analysis. European Respiratory Journal 54:1801991.

15. Koh WJ, Stout JE, Yew WW. 2014. Advances in the management of pulmonary disease due to Mycobacterium abscessus complex. Int J Tuberc Lung Dis 18:1141-8.

16. Kwak N, Dalcolmo MP, Daley CL, Eather G, Gayoso R, Hasegawa N, Jhun BW, Koh WJ, Namkoong H, Park J, Thomson R, van Ingen J, Zweijpfenning SMH, Yim JJ. 2019. M ycobacterium abscessus pulmonary disease: individual patient data meta-analysis. Eur Respir J 54.

17. Woods GL, Brown-Elliott BA, Conville PS, Desmond EP, Hall GS, Lin G, Pfyffer GE, Ridderhof JC, Siddiqi SH, Wallace RJ, Jr., Warren NG, Witebsky FG. 2011. CLSI Standards: Guidelines for Health Care Excellence, Susceptibility Testing of Mycobacteria, Nocardiae, and Other Aerobic Actinomycetes. Clinical and Laboratory Standards Institute

18. Cokol M, Kuru N, Bicak E, Larkins-Ford J, Aldridge BB. 2017. Efficient measurement and factorization of high-order drug interactions in Mycobacterium tuberculosis</em&gt. Science Advances 3:e1701881.

19. Cho YJ, Yi H, Chun J, Cho SN, Daley CL, Koh WJ, Shin SJ. 2013. The genome sequence of 'Mycobacterium massiliense' strain CIP 108297 suggests the independent taxonomic status of the Mycobacterium abscessus complex at the subspecies level. PLoS One 8:e81560.

20. Vaara M, Siikanen O, Apajalahti J, Fox J, Frimodt-Moller N, He H, Poudyal A, Li J, Nation RL, Vaara T. 2010. A novel polymyxin derivative that lacks the fatty acid tail and carries only three positive charges has strong synergism with agents excluded by the intact outer membrane. Antimicrob Agents Chemother 54:3341-6.

21. Vaara M. 2013. Novel derivatives of polymyxins. J Antimicrob Chemother 68:1213-9.

22. Corbett D, Wise A, Langley T, Skinner K, Trimby E, Birchall S, Dorali A, Sandiford S, Williams J, Warn P, Vaara M, Lister T. 2017. Potentiation of Antibiotic Activity by a Novel Cationic Peptide: Potency and Spectrum of Activity of SPR741. Antimicrobial agents and chemotherapy 61:e00200-17.

23. Viljoen A, Raynaud C, Johansen MD, Roquet-Banères F, Herrmann J-L, Daher W, Kremer L. 2019. Verapamil Improves the Activity of Bedaquiline against Mycobacterium abscessus In Vitro and in Macrophages. Antimicrobial agents and chemotherapy 63:e00705-19.

24. Chen J, Zhao L, Mao Y, Ye M, Guo Q, Zhang Y, Xu L, Zhang Z, Li B, Chu H. 2019. Clinical Efficacy and Adverse Effects of Antibiotics Used to Treat Mycobacterium abscessus Pulmonary Disease. Frontiers in microbiology 10:1977-1977.

25. Griffith DE. 1999. Risk-Benefit Assessment of Therapies for Mycobacterium avium Complex Infections. Drug Safety 21:137-152.

26. Brown-Elliott BA, Nash KA, Wallace RJ, Jr. 2012. Antimicrobial susceptibility testing, drug resistance mechanisms, and therapy of infections with nontuberculous mycobacteria. Clinical microbiology reviews 25:545-582.

27. Lindman M, Dick T. Bedaquiline Eliminates Bactericidal Activity of β-Lactams against Mycobacterium abscessus. Antimicrobial Agents and Chemotherapy 63:e00827-19.

28. Zhang Z, Lu J, Song Y, Pang Y. 2018. In vitro activity between linezolid and other antimicrobial agents against Mycobacterium abscessus complex. Diagn Microbiol Infect Dis 90:31-34.

29. Pryjma M, Burian J, Thompson CJ. 2018. Rifabutin Acts in Synergy and Is Bactericidal with Frontline Mycobacterium abscessus Antibiotics Clarithromycin and Tigecycline, Suggesting a Potent Treatment Combination. Antimicrob Agents Chemother 62.

30. Larkins-Ford J, Greenstein T, Van N, Degefu YN, Olson MC, Sokolov A, Aldridge BB. 2021. Systematic measurement of combination-drug landscapes to predict in vivo treatment outcomes for tuberculosis. Cell Systems 12:1046-1063.e7.

949 31. Griffith DE, Aksamit T, Brown-Elliott BA, Catanzaro A, Daley C, Gordin F, Holland
950 SM, Horsburgh R, Huitt G, Iademarco MF, Iseman M, Olivier K, Ruoss S, von Reyn
951 CF, Wallace RJ, Jr., Winthrop K. 2007. An official ATS/IDSA statement: diagnosis,
952 treatment, and prevention of nontuberculous mycobacterial diseases. Am J Respir Crit
953 Care Med 175:367-416.

954 32. Lindman M, Dick T. 2019. Bedaquiline Eliminates Bactericidal Activity of beta-
955 Lactams against Mycobacterium abscessus. Antimicrob Agents Chemother 63.

956 33. Sarathy JP, Gruber G, Dick T. 2019. Re-Understanding the Mechanisms of Action of
957 the Anti-Mycobacterial Drug Bedaquiline. Antibiotics (Basel) 8.

958 34. Nie W, Duan H, Huang H, Lu Y, Bi D, Chu N. 2014. Species identification of
959 Mycobacterium abscessus subsp. abscessus and
960 Mycobacterium abscessus subsp. bolletii using
961 rpoB and hsp65, and susceptibility testing to eight antibiotics.
962 International Journal of Infectious Diseases 25:170-174.

963 35. Choi G-E, Min K-N, Won C-J, Jeon K, Shin SJ, Koh W-J. 2012. Activities of
964 moxifloxacin in combination with macrolides against clinical isolates of
965 Mycobacterium abscessus and Mycobacterium massiliense. Antimicrobial agents and
966 chemotherapy 56:3549-3555.

967 36. Moon SM, Park HY, Kim SY, Jhun BW, Lee H, Jeon K, Kim DH, Huh HJ, Ki CS,
968 Lee NY, Kim HK, Choi YS, Kim J, Lee SH, Kim CK, Shin SJ, Daley CL, Koh WJ.
969 2016. Clinical Characteristics, Treatment Outcomes, and Resistance Mutations
970 Associated with Macrolide-Resistant Mycobacterium avium Complex Lung Disease.
971 Antimicrob Agents Chemother 60:6758-6765.

972 37. Ganapathy US, Rio RGd, Cacho-Izquierdo M, Ortega F, Lelièvre J, Barros-Aguirre D,
973 Lindman M, Dartois V, Gengenbacher M, Dick T. 2021. A Leucyl-tRNA Synthetase
974 Inhibitor with Broad-Spectrum Antimycobacterial Activity. Antimicrobial Agents and
975 Chemotherapy 65:e02420-20.

976 38. Rominski A, Roditscheff A, Selchow P, Böttger EC, Sander P. 2017. Intrinsic
977 rifamycin resistance of Mycobacterium abscessus is mediated by ADP-
978 ribosyltransferase MAB_0591. J Antimicrob Chemother 72:376-384.

979 39. Ganapathy US, Dartois V, Dick T. 2019. Repositioning rifamycins for
980 Mycobacterium abscessus lung disease. Expert Opin Drug Discov 14:867-878.

981 40. Becker K, Haldimann K, Selchow P, Reinau LM, Dal Molin M, Sander P. 2017.
982 Lipoprotein Glycosylation by Protein-O-Mannosyltransferase (MAB_1122c)
983 Contributes to Low Cell Envelope Permeability and Antibiotic Resistance of
984 Mycobacterium abscessus. Front Microbiol 8:2123.

985 41. Baysarowich J, Koteva K, Hughes DW, Ejim L, Griffiths E, Zhang K, Junop M,
986 Wright GD. 2008. Rifamycin antibiotic resistance by ADP-ribosylation: Structure and
987 diversity of Arr. Proc Natl Acad Sci U S A 105:4886-91.

988 42. Paulowski L, Beckham KSH, Johansen MD, Berneking L, Van N, Degefu Y, Staack
989 S, Sotomayor FV, Asar L, Rohde H, Aldridge BB, Aepfelbacher M, Parret A,
990 Wilmanns M, Kremer L, Combrink K, Maurer FP. 2022. C25-modified rifamycin
991 derivatives with improved activity against Mycobacterium abscessus. PNAS Nexus 1.

992 43. Pryjma M, Burian J, Thompson CJ. 2018. Rifabutin Acts in Synergy and Is
993 Bactericidal with Frontline Mycobacterium abscessus Antibiotics Clarithromycin and
994 Tigecycline, Suggesting a Potent Treatment Combination. Antimicrobial Agents and
995 Chemotherapy 62:e00283-18.

996 44. Fernández-Roblas R, Esteban J, Cabria F, López JC, Jiménez MS, Soriano F. 2000. In
997 vitro susceptibilities of rapidly growing mycobacteria to telithromycin (HMR 3647)
998 and seven other antimicrobials. Antimicrob Agents Chemother 44:181-2.

999 45. van der Paardt A-F, Wilffert B, Akkerman OW, de Lange WCM, van Soolingen D,
1000 Sinha B, van der Werf TS, Kosterink JGW, Alffenaar J-WC. 2015. Evaluation of
1001 macrolides for possible use against multidrug-resistant Mycobacterium
1002 tuberculosis. European Respiratory Journal 46:444-455.

1003 46. Kannan K, Vázquez-Laslop N, Mankin AS. 2012. Selective protein synthesis by
1004 ribosomes with a drug-obstructed exit tunnel. Cell 151:508-20.

1005 47. Clay KD, Hanson JS, Pope SD, Rissmiller RW, Purdum PP, 3rd, Banks PM. 2006.
1006 Brief communication: severe hepatotoxicity of telithromycin: three case reports and
1007 literature review. Ann Intern Med 144:415-20.

1008 48. Lopeman RC, Harrison J, Rathbone DL, Desai M, Lambert PA, Cox JAG. 2020.
1009 Effect of Amoxicillin in combination with Imipenem-Relebactam against
1010 Mycobacterium abscessus. Scientific reports 10:928-928.

1011 49. Mukherjee D, Wu ML, Teo JWP, Dick T. 2017. Vancomycin and Clarithromycin
1012 Show Synergy against Mycobacterium abscessus In Vitro. Antimicrob Agents
1013 Chemother 61.

1014 50. Dupont C, Viljoen A, Thomas S, Roquet-Banères F, Herrmann J-L, Pethe K, Kremer
1015 L. 2017. Bedaquiline Inhibits the ATP Synthase in Mycobacterium abscessus and Is
1016 Effective in Infected Zebrafish. Antimicrobial agents and chemotherapy 61:e01225-
1017 17.

1018 51. Philley JV, Wallace RJ, Jr., Benwill JL, Taskar V, Brown-Elliott BA, Thakkar F,
1019 Aksamit TR, Griffith DE. 2015. Preliminary Results of Bedaquiline as Salvage
1020 Therapy for Patients With Nontuberculous Mycobacterial Lung Disease. Chest
1021 148:499-506.

1022 52. Lindman M, Dick T. 2019. Bedaquiline Eliminates Bactericidal Activity of β-Lactams
1023 against Mycobacterium abscessus. Antimicrob Agents Chemother 63.

1024 53. Erber J, Weidlich S, Tschaikowsky T, Rothe K, Schmid RM, Schneider J, Spinner CD.
1025 2020. Successful bedaquiline-containing antimycobacterial treatment in post-
1026 traumatic skin and soft-tissue infection by Mycobacterium fortuitum complex: a case
1027 report. BMC Infectious Diseases 20:365.

1028 54. Chohan PS, Mittal R, Javed A. 2015. Antipsychotic Medication and QT Prolongation.
1029 Pakistan journal of medical sciences 31:1269-1271.

1030 55. Amaral L, Viveiros M. 2017. Thioridazine: A Non-Antibiotic Drug Highly Effective,
1031 in Combination with First Line Anti-Tuberculosis Drugs, against Any Form of
1032 Antibiotic Resistance of Mycobacterium tuberculosis Due to Its Multi-Mechanisms of
1033 Action. Antibiotics (Basel, Switzerland) 6:3.

1034 56. Cantelli CR, Dassonville-Klimpt A, Sonnet P. 2021. A review of current and
1035 promising nontuberculous mycobacteria antibiotics. Future Medicinal Chemistry
1036 13:1367-1395.

1037 57. Chopra S, Matsuyama K, Tran T, Malerich JP, Wan B, Franzblau SG, Lun S, Guo H,
1038 Maiga MC, Bishai WR, Madrid PB. 2012. Evaluation of gyrase B as a drug target in
1039 Mycobacterium tuberculosis. J Antimicrob Chemother 67:415-21.

1040 58. Locher CP, Jones SM, Hanzelka BL, Perola E, Shoen CM, Cynamon MH, Ngwane
1041 AH, Wiid IJ, van Helden PD, Betoudji F, Nuermberger EL, Thomson JA. 2015. A
1042 novel inhibitor of gyrase B is a potent drug candidate for treatment of tuberculosis and
1043 nontuberculosis mycobacterial infections. Antimicrob Agents Chemother 59:1455-65.

1044 59. Novosad SA, Beekmann SE, Polgreen PM, Mackey K, Winthrop KL, Team MaS.
1045 2016. Treatment of Mycobacterium abscessus Infection. Emerg Infect Dis 22:511-4.

1046 60. Von Döhren H. 2004. Antibiotics: Actions, origins, resistance, by C. Walsh. 2003.
1047 Washington, DC: ASM Press. 345 pp. $99.95 (hardcover). Protein Science 13:3059-
1048 3060.

1049 61. Lefebvre A-L, Le Moigne V, Bernut A, Veckerlé C, Compain F, Herrmann J-L,
1050 Kremer L, Arthur M, Mainardi J-L. 2017. Inhibition of the β-Lactamase Bla(Mab) by
1051 Avibactam Improves the In Vitro and In Vivo Efficacy of Imipenem against
1052 Mycobacterium abscessus. Antimicrobial agents and chemotherapy 61:e02440-16.

1053 62. Nguyen L, Thompson CJ. 2006. Foundations of antibiotic resistance in bacterial
1054 physiology: the mycobacterial paradigm. Trends in Microbiology 14:304-312.

1055 63. Dubée V, Bernut A, Cortes M, Lesne T, Dorchene D, Lefebvre AL, Hugonnet JE,
1056 Gutmann L, Mainardi JL, Herrmann JL, Gaillard JL, Kremer L, Arthur M. 2015. β-
1057 Lactamase inhibition by avibactam in Mycobacterium abscessus. J Antimicrob
1058 Chemother 70:1051-8.

1059 64. Baky SH, Singh BN. 1982. Verapamil hydrochloride: pharmacological properties and
1060 role in cardiovascular therapeutics. Pharmacotherapy 2:328-353.

1061 65. van Heeswijk RPG, Dannemann B, Hoetelmans RMW. 2014. Bedaquiline: a review
1062 of human pharmacokinetics and drug–drug interactions. Journal of Antimicrobial
1063 Chemotherapy 69:2310-2318.

1064 66. Plana D, Palmer AC, Sorger PK. 2022. Independent Drug Action in Combination
1065 Therapy: Implications for Precision Oncology. Cancer Discovery 12:606-624.

1066 67. Aono A, Morimoto K, Chikamatsu K, Yamada H, Igarashi Y, Murase Y, Takaki A,
1067 Mitarai S. 2019. Antimicrobial susceptibility testing of Mycobacteroides

(Mycobacterium) abscessus complex, Mycolicibacterium (Mycobacterium) fortuitum, and Mycobacteroides (Mycobacterium) chelonae. Journal of Infection and Chemotherapy 25:117-123.

68. McNeil MB, Chettiar S, Awasthi D, Parish T. 2019. Cell wall inhibitors increase the accumulation of rifampicin in Mycobacterium tuberculosis. Access Microbiol 1:e000006.

69. Wu ML, Aziz DB, Dartois V, Dick T. 2018. NTM drug discovery: status, gaps and the way forward. Drug Discov Today 23:1502-1519.

70. Kreutzfeldt KM, McAdam PR, Claxton P, Holmes A, Seagar AL, Laurenson IF, Fitzgerald JR. 2013. Molecular Longitudinal Tracking of Mycobacterium abscessus spp. during Chronic Infection of the Human Lung. PLOS ONE 8:e63237.

71. Lázár V, Snitser O, Barkan D, Kishony R. 2022. Antibiotic combinations reduce Staphylococcus aureus clearance. Nature 610:540-546.

72. Nuermberger EL. 2017. Preclinical Efficacy Testing of New Drug Candidates. Microbiol Spectr 5.

73. Parish T. 2020. In vitro drug discovery models for Mycobacterium tuberculosis relevant for host infection. Expert Opin Drug Discov 15:349-358.

74. Larkins-Ford J, Degefu YN, Van N, Sokolov A, Aldridge BB. 2021. Design principles to assemble drug combinations for effective tuberculosis therapy using interpretable pairwise drug response measurements. bioRxiv doi:10.1101/2021.12.05.471248:2021.12.05.471248.

75. Lee J, Ammerman N, Agarwal A, Naji M, Li SY, Nuermberger E. 2021. Differential In Vitro Activities of Individual Drugs and Bedaquiline-Rifabutin Combinations against Actively Multiplying and Nutrient-Starved Mycobacterium abscessus. Antimicrob Agents Chemother 65.

76. Hunt-Serracin AC, Parks BJ, Boll J, Boutte CC. 2019. Mycobacterium abscessus Cells Have Altered Antibiotic Tolerance and Surface Glycolipids in Artificial Cystic Fibrosis Sputum Medium. Antimicrob Agents Chemother 63.

77. Davidson RM, Hasan NA, Reynolds PR, Totten S, Garcia B, Levin A, Ramamoorthy P, Heifets L, Daley CL, Strong M. 2014. Genome sequencing of Mycobacterium

abscessus isolates from patients in the united states and comparisons to globally diverse clinical strains. J Clin Microbiol 52:3573-82.

78. Van N, Degefu YN, Aldridge BB. 2021. Efficient Measurement of Drug Interactions with DiaMOND (Diagonal Measurement of N-Way Drug Interactions). Methods Mol Biol 2314:703-713.

79. Gadagkar SR, Call GB. 2015. Computational tools for fitting the Hill equation to dose-response curves. J Pharmacol Toxicol Methods 71:68-76.

80. Baeder DY, Yu G, Hoze N, Rolff J, Regoes RR. 2016. Antimicrobial combinations: Bliss independence and Loewe additivity derived from mechanistic multi-hit models. Philos Trans R Soc Lond B Biol Sci 371.

81. Maurer FP, Castelberg C, Quiblier C, Bottger EC, Somoskovi A. 2014. Erm(41)-dependent inducible resistance to azithromycin and clarithromycin in clinical isolates of Mycobacterium abscessus. J Antimicrob Chemother 69:1559-63.